Desalination and Water Treatment
www.deswater.com
doi: 10.5004/dwt.2019.23408

142 (2019) 235–243
February

Characteristics and mechanisms of molybdenum(VI) adsorption by drinking water treatment residue

Jian-jun Lian[a], Mei Yang[a], Bo Chen[a,*], Shi-sheng Wang[a], Tian-ran Ye[a], Dong-dong Zheng[a], Chuan-rui Jiang[b]

[a]*College of Energy and Environment, Anhui University of Technology, Anhui 243002, China, Tel. +86 0555 2312885; emails: greenchenbo@163.com (B. Chen), jjlian85@126.com (J.-j. Lian), 15755505979@163.com (M. Yang), ahutsswang@163.com (S.-s. Wang), natureye66@163.com (T.-r. Ye), zdd1570197377@163.com (D.-d. Zheng)*
[b]*Department of Environmental Science, Guangdong Polytechnic of Environmental Protection Engineering, Guangzhou 528216, China, email: jiang.cr@hotmail.com*

Received 31 March 2018; Accepted 31 October 2018

ABSTRACT

Molybdenum (Mo) is an important pollutant in surface water. Removal of Mo from aqueous solutions by adsorption using low-cost and environmental friendly adsorbents has gained wide acceptance. Drinking water treatment residue (DWTR) is an inevitable by-product during potable water production that has the high capability of adsorption of heavy metals. However, the characteristics and mechanisms of Mo adsorption by DWTR still remain unclear. In this study, we showed that Mo(VI) adsorption by DWTR followed the pseudo-second-order rate. The adsorption isotherms for Mo(VI) were best described by the Langmuir model. Thermodynamic parameters indicated that the adsorption process was endothermal, entropy increasing, and spontaneous. Electrostatic interaction and surface complexation were found to be major adsorption mechanisms. The adsorption rate of Mo(VI) by DWTR was dependent on pH values and lineally increased as pH decreased from 10 to 4. The estimated maximum adsorption capacity was 31.06 mg/g at 318 K at pH 2.0. Desorption experiments were also performed to evaluate the potential of DWTR regeneration. These results suggested that DWTR was a green, efficient, and recyclable adsorbent for Mo(VI) and could be used for removal and recovery of Mo from polluted environments.

Keywords: Mo; DWTR; Adsorption; Desorption; Isotherms

1. Introduction

Molybdenum (Mo) is a key micronutrient for both plants and animals and has long been known as one of the biologically active transition elements [1,2]. The provisional dietary intake recommended is 75–250 μg/d for adults and older children [3]. However, it would become toxic when Mo concentration in water is over 5 mg/L, and the toxic degree of molybdate compounds ranks between those of Zn(II) and Cr(III) compounds [4]. Notably, due to the huge Mo effluents from mining tailings without any pretreatment, Mo pollution of surface waters has become an important environmental problem [5], and Mo pollution events have been reported around the world, such as in Brenda Mines in British Columbia, Canada; the San Joaquin Valley, USA; and in Wujintang Reservoir, China [6]. Mo can exist in various oxidation states ranging from +2 to +6 in water solution, while molybdate ion (MoO_4^{2-}) is the most soluble species, and is widely distributed in natural environment and wastewater [7]. Therefore, removal of MoO_4^{2-} from aqueous solutions is of significant importance from an environmental point of view. From an economic standpoint, its recovery would also be attractive because Mo is a precious metal with many industrial applications.

* Corresponding author.

Methods, e.g., ion exchange [8], chemical precipitation [9], and adsorption [10], have been developed for Mo pollution control in aqueous solutions, and most of them have been demonstrated to be effective under various environmental conditions. Among these methods, adsorption gained wide acceptance because it was an efficient and economically feasible process for purification [11]. Reasonably, a low-cost and environmental friendly adsorbent with high adsorption capability can promote the application of Mo adsorption for environmental remediation. Many studies have found that iron and aluminum oxide-based adsorbents were feasible for Mo(VI) removal [12,13]. Interestingly, recycling of drinking water treatment residue (DWTR), a by-product containing relatively high Al and Fe contents, for adsorbents has received increasing attentions from scientists [14,15].

DWTR is an inevitable and nonhazardous by-product generated hugely during potable water production. The high contents of Al and Fe from DWTR were mainly from the used flocculants for water purification and existed as amorphous forms, endowing DWTR with high adsorption capability [16]. It has been reported that DWTR exhibits high capability to adsorb Co [14], Cu [15], As [17], and Hg [18]. Accordingly, we hypothesize that DWTR can also be a good material for Mo adsorption from aqueous solutions. However, due to lack of a sustainable application, DWTRs are mainly disposed by landfilling with high cost [19]. Successful development of an Mo adsorbent based on DWTR would lead to a win-win method for environmental remediation.

Therefore, adsorption of Mo(VI) from aqueous solution by using DWTR was investigated in this study. The adsorption kinetics, equilibrium studies, the effects of pH and temperature, and the binding mechanism were particularly investigated. The stability of adsorbed Mo was also determined based on desorption tests. The results will provide important information on the recycling of DWTR and its application in the removal of heavy metals from aqueous solution.

2. Materials and methods

2.1. Chemicals and materials

Sodium molybdate 2-hydrate ($Na_2MoO_4 \cdot 2H_2O$) was employed to prepare a stock solution containing 1,000 mg/L of Mo(VI), which was further diluted with deionized water to desired quantity. The DWTRs were collected from the Capital water treatment plant in Maanshan, China, which primarily treats surface waters from the Changjiang River. Moreover, Fe and Al salts are the primary coagulants used in the water treatment process. Fresh DWTR samples were air-dried, ground, and sieved (<0.15 mm) prior to use. Distilled water was used throughout the entire experiment. All reagents were of analytical grade and were used without further purification.

2.2. Batch experiments for Mo(VI) adsorption

Batch adsorption experiments were carried out by agitating 0.1 g of DWTR with 100 mL aqueous solution of 0–100 mg/L Mo(VI) in a shake table. The ionic strength (0.1 mol/L NaCl) of the Mo(VI) solution was adjusted to constant value. Continuous shaking was provided during the experiments with a constant agitation speed of 180 rpm. Blanks were carried out with the same procedures as the samples. All the experiments were repeated three times. The data presented in both the tables and figures are average values. The Mo concentrations adopted here were mainly based on wastewaters, in which the dissolved Mo could be as high as 30 mg/L [20].

The adsorption kinetics experiment was carried out at an optimum pH with an initial concentration of 50 mg/L for different time intervals. Isotherm studies were performed with concentrations of Mo(VI) from 2 to 100 mg/L at varying temperatures of 25°C, 35°C, and 45°C. The shaking time was 24 h, which was the optimum time determined by the kinetics experiments. At the end of the adsorption equilibration time, the suspensions were filtered through 0.45 μm pore size filters, and the residual molybdate ion was analyzed.

The effect of pH was investigated by adding 0.1 g of DWTR into 100 mL aqueous solution of 10 mg/L Mo(VI). The pH of the solutions was adjusted to 1.0–10.0 before being mixed with the DWTR. After mixture, all the samples were shaken for 24 h at 25°C. Both Mo(VI) concentration in the solution and pH after adsorption were measured. The initial pH of the mineral suspensions containing Mo(VI) was adjusted to the range of 1.0–10.0 using 1 mol/L HCl or 1 mol/L NaOH additions, and the changed total volume was <2%. The point of zero charge (PZC) of the material was tested by the mass titration method, which demonstrated that the pH of the system will approach $pH_\infty = (pK_1 + pK_2)_{PZC}/2$ under the limiting conditions of "infinite" mass/volume ratio [21]. Percentage adsorption (%A) for Mo was calculated according to Eq. (1):

$$\%A = \frac{\left(C_i - C_e\right)}{C_i} \times 100 \tag{1}$$

where C_i is the initial concentration of Mo(VI) and C_e stands for the equilibrium concentration measured after adsorption on the DWTR.

2.3. Desorption studies

Desorption experiments were conducted by adding 1 g of DWTR to 1,000 mL aqueous solution of 10 mg/L Mo(VI), followed by stirring for 24 h at 25°C. After adsorption, the suspensions were filtered and the Mo(VI) concentration was analyzed. After being washed three times with deionized water, the residuals were dried overnight at 105°C and stocked in glass bottles. Then, 0.1 g samples were suspended in 100 mL distilled water with six concentrations of NaOH solutions (0.001, 0.01, 0.05, 0.1, 0.5, and 1 mol/L). The suspensions were shaken for 5 h (desorption equilibrium was reached within 5 h) and centrifuged. The desorption efficiency was calculated from the amount of Mo released into the solutions.

2.4. Analyses

The structure and surface characteristics of adsorbents were measured using scanning electron microscopy (SEM) (Hitachi S-4800, Japan). Specific surface area was measured by Brunauer-Emmett-Teller method using Micromeritics

Tristar 3020. The elemental properties of the DWTR were analyzed using an ARL ADVANTX Intellipower™ 3600 device (X-ray fluorescence (XRF), Thermo Fisher Co., Switzerland). Powder X-ray diffraction (XRD) patterns at 2θ angles from 10° to 80° were recorded at an interval of 0.33° on an UItima IV diffractometer using Cu radiation (40 kV, 40 mA). Fourier-transform infrared spectroscopy (FTIR) spectra were recorded on a Nicolet 6700 FTIR spectrophotometer. The X-ray photoelectron spectroscopy (XPS) analysis was taken by an XPS Escalab 250Xi with the monochromatic Al Kα X-ray radiation. The pH value of the solution was measured by S-3C model pH meter, while the concentrations of molybdate were measured by using PE AA700 model atomic absorption spectrophotometer.

3. Results and discussion

3.1. Characterization of the DWTR

SEM and XRD analyses showed that the original DWTR was porous and amorphous with a rough surface (Fig. 1(a)), which was consistent with reported findings by Quinones [18]. XRF analysis showed that the original DWTRs contain predominantly high levels of Si, Al, and Fe contents of 41.1%, 30.8%, and 17.2%, respectively, and relatively small amounts of Ca, K, Mg, and other elements. XRD patterns of the DWTR did not reveal many sharp diffraction characteristic peaks over a broad range of *d*-spacings (10°–80°, 2θ), indicating that they were primarily short-range-ordered materials (Fig. 1(b)). However, XRD spectra for DWTR showed some sharp peaks that can be attributed to the presence of quartz and other weak peaks of mostly unidentified minerals. The surface area of the DWTR was 64.58 m^2/g (particle size < 0.15 mm), which is close to the findings of other authors [14].

3.2. Adsorption kinetics of Mo(VI) adsorption on DWTR

Adsorption kinetics can provide valuable insight into the reaction pathways and mechanisms. The results showed that the adsorption kinetics included a rapid initial adsorption followed by a smooth increase, with equilibrium reached in less than 24 h (Fig. 2). Then, four common kinetic models

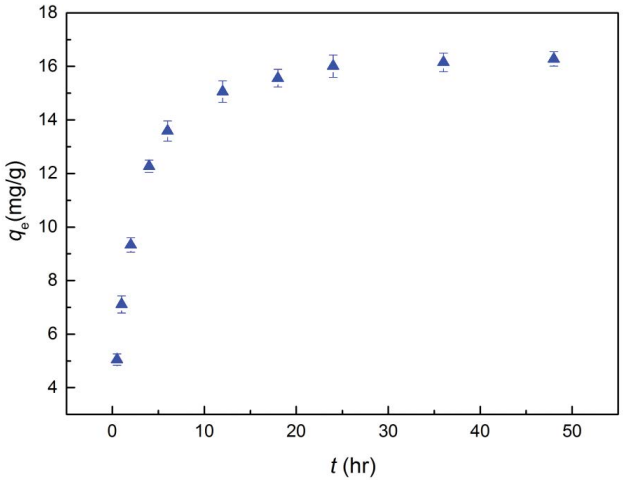

Fig. 2. Adsorption kinetic data for Mo(VI) on DWTR. Conditions: Solid/liquid = 1 g/L, temperature = 298 K, initial Mo concentration = 50 mg/L, pH = 2.0.

such as the pseudo-first-order model, pseudo-second-order model, Elovich mass transfer model, and intraparticle diffusion model were employed to describe the adsorption process of Mo(VI) on DWTR.

The pseudo-first-order model is used when the rate of occupation of binding sites is proportional to the number of unoccupied sites on the biosorbent. The pseudo-second-order model is applied when the rate of occupation of adsorption sites is proportional to the square of the number of unoccupied sites on the biosorbent [22]. The Elovich equation and intraparticle diffusion equation are used to identify the importance of diffusion in the sorption process. The expression formulas and the correlative parameters of these kinetic models with the correlation coefficients (R^2) were represented in Table 1.

It can be seen from Table 1 that the correlation coefficient for the second-order kinetic equation was approximately 0.993. The calculated q_e values also agree well with the experimental data (q_{exp} = 16.28 mg/g). Such information indicated that

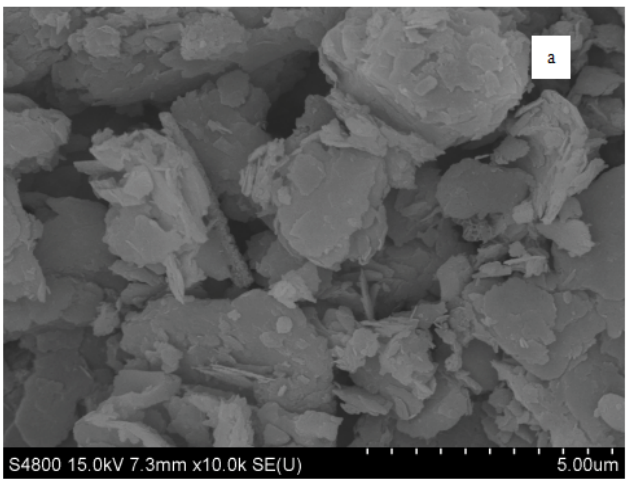

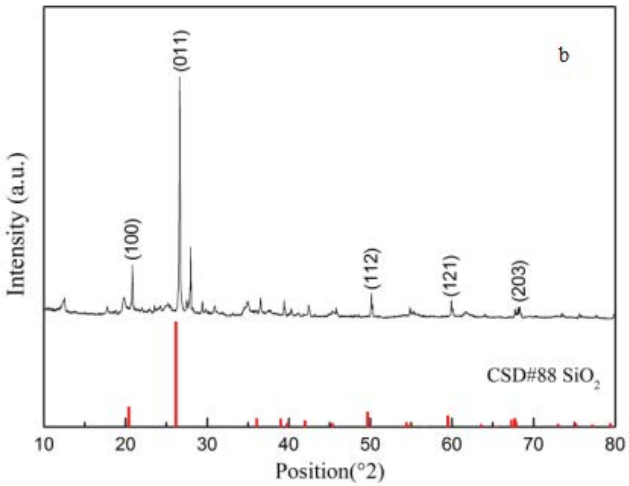

Fig. 1. SEM analysis of DWTR (a) and XRD patterns of DWTR (b).

Table 1
Comparison of the four kinetic models for Mo(VI) adsorption on DWTR at 298 K.

Kinetic models	Expression formula	Parameters	298 K
Pseudo-first-order	$\ln\left(q_e - q_t\right) = \ln q_e - k_1 t$	q_e (mg/g)	15.30
		k_1 (1/min)	0.51
		R^2	0.932
Pseudo-second-order	$\frac{t}{q_t} = \frac{1}{k_2 q_e^2} + \frac{t}{q_e}$	q_e (mg/g)	16.74
		k_2 (mg/g min)	0.04
		R^2	0.993
Elovich mass transfer	$q_t = \beta \ln\left(\alpha\beta\right) + \beta \ln\left(t\right)$	α (mg/g min)	6.95
		β (g/mg)	2.63
		R^2	0.939
Intraparticle diffusion	$q_t = k_{dif} t^{1/2} + d$	k_{dif} (mg/g min$^{1/2}$)	1.69
		d (mg/g)	7.01
		R^2	0.691

adsorption of Mo(VI) onto the DWTR is best represented by the pseudo-second-order kinetic model, based on the assumption that the rate-limiting step may be chemical sorption or chemisorption involving valency forces through sharing or exchange of electrons between adsorbate and adsorbent [10].

In the case of the Elovich equation, the correlation coefficients are lower than those of the pseudo-second-order equation. Elovich equation is useful in describing adsorption on highly heterogeneous adsorbents, but this situation indicates that the Elovich equation might not be sufficient to describe the mechanism. The intraparticle diffusion model could not well describe the adsorption (R^2 = 0.691, compared with other models) suggested that the intraparticle diffusion may not be the rate controlling factor in determining the kinetics of the process [23].

3.3. Adsorption isotherms on DWTR

The adsorption isotherms express the specific relation between the concentration of the adsorbate and its degree of accumulation onto adsorbent surface at constant temperature [11]. Several isotherm models were used to fit to the experimental data and evaluate the isotherm performance for Mo(VI) adsorption. These isotherm models include Langmuir isotherm, Freundlich isotherm, Temkin isotherm, and Dubinin-Radushkevich isotherm, and these equations were expressed in our previous work [6]. The adsorption isotherms and the fitting model parameters with R^2 for the different models are shown in Fig. 3 and Table 2.

It can be seen that the Mo adsorption contents by DWTR increased as the initial concentrations increased, and the Langmuir isotherm model showed the best fit to adsorption data than the other isotherm equations in terms of coefficient. The fact that the Langmuir isotherm can well describe the adsorption may be due to homogenous distribution of active sites on the adsorbent surface. A further comparison of the Mo(VI) adsorption capacity of some adsorbents based on the values of Q_0 (Table 3) indicated that the present adsorbent has high adsorption capacity (24.43–31.06 mg/g) in comparison with the reported adsorbents.

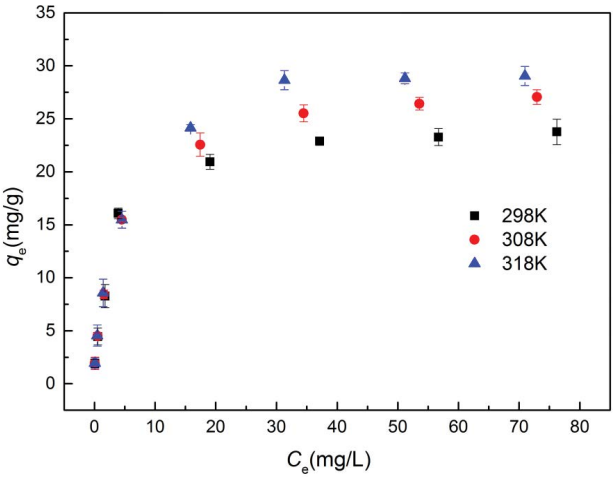

Fig. 3. Adsorption isotherm data for Mo(VI) on DWTR. Conditions: Solid/liquid = 1 g/L, shaking time = 24 h, pH = 2.0.

From the Temkin isotherms, typical bonding energy range for the ion-exchange mechanism was reported to be in the range of 8–16 kJ/mol while the physic-sorption process was reported to have adsorption energies less than −40 kJ/mol [24]. The value of b_T (3.60–4.55 kJ/mol) obtained in the present study indicated that the adsorption process seemed to be involved in the chemisorption and physic-sorption.

3.4. Thermodynamics of Mo(VI) adsorption on DWTR

Temperature is one of major factors affecting adsorption process. The Mo(VI) adsorption by DWTR was determined at three different temperatures (298, 308, and 318 K). The thermodynamic parameters such as Gibbs free energy change ($\Delta G°$), enthalpy change ($\Delta H°$), and entropy change ($\Delta S°$) were calculated using the following equations:

$$\Delta G° = -RT \ln K_{ad} \quad (2)$$

Table 2
Isotherm model parameters for Mo(VI) adsorption to DWTR at three temperatures.

Isotherm models	Expression formula	Parameters	298 K	308 K	318 K
Langmuir	$\frac{C_e}{q_e}=\frac{C_e}{Q_0}+\frac{1}{Q_0 b}$	Q_0 (mg/g)	24.43	28.03	31.06
		b (L/mg)	0.38	0.28	0.25
		R^2	0.988	0.995	0.992
Freundlich	$\ln q_e=\frac{1}{n}\ln C_e+\ln k_F$	k_F (mg^{1-n} L^n/g)	8.45	8.12	8.73
		n	0.26	0.29	0.29
		R^2	0.903	0.951	0.947
Temkin	$q_e=\frac{RT}{b_T}\ln A+\frac{RT}{b_T}\ln C_e$	A (L/g)	12.28	9.34	9.75
		b_T (kJ/mol)	3.60	4.16	4.55
		R^2	0.949	0.960	0.946
Dubinin-Radushkevich	$\ln Q_e=\ln Q_m-\beta\varepsilon^2$	Q_m (mg/g)	22.64	24.85	26.91
		$B\times10^{-2}$ (mol^2/kJ^2)	0.096	0.107	0.111
		R^2	0.942	0.909	0.891

Table 3
Comparison between the adsorption of Mo(VI) by DWTR and other adsorbents reported in literature

Adsorbents	Adsorption capacity (mg/g)	References
Nano-magnetic $CuFe_2O_4$	30.58	[25]
Maghemite nanoparticles	33.4	[1]
NaOCl-oxidized multiwalled carbon nanotubes	22.73	[26]
Carminic acid-modified anion exchanger	13.5	[27]
Zeolite-supported magnetite	18.0	[28]
Hydrotalcite-like layered double hydroxides	16.2	[29]
Drinking water treatment residue	24.43–31.06	Present

$$\ln K_{ad}=\frac{\Delta S^\circ}{R}-\frac{\Delta H^\circ}{RT} \tag{3}$$

where R is the gas constant (8.314 J/(mol K)), T is the absolute temperature (K), and K_{ad} is the adsorption equilibrium constant. Then the Gibbs free energy of adsorption (ΔG°) is determined from Eq. (2). Plotting $\ln K_{ad}$ against $1/T$ gives a straight line with slope and intercept equal to $\Delta H^\circ/R$ and $\Delta S^\circ/R$, respectively; see Eq. (3).

The values of ΔG°, ΔH°, and ΔS° for Mo(VI) adsorption on the DWTR have been calculated and are shown in Table 4. The value of ΔH° was positive in the process of Mo(VI) adsorbed on DWTR, suggesting that the adsorption process is endothermic and temperature dependent. The positive value of ΔS° showed the increased randomness at the solid/solution interface during the Mo(VI) adsorption. The negative values of ΔG° indicated that the adsorption process was spontaneous in nature. Moreover, the decrease in ΔG° values with increasing temperature suggested that the adsorption process is favorable at high temperatures. The ΔG° values obtained in this study for Mo(VI) were less than −10 kJ/mol, suggesting that the physical adsorption mechanism existed in the adsorption process.

3.5. Desorption studies

Desorption experiments were performed to evaluate the potential of DWTR regeneration. It indicated the Mo desorption rate above 60% under investigated NaOH concentrations (Fig. 4(a)). The desorbed amount of Mo increased along with NaOH concentrations, from 65.31% to 81.85%. Moreover, 0.05 mol/L NaOH solution is sufficient for Mo desorption. Desorption of Mo resulted from the displacement of Mo from the adsorbent sites by OH^- ions [30]. In addition, three cycles of adsorption-desorption experiments were carried out to investigate the regeneration of DWTR for Mo(VI) removal efficiency. The results showed that about 75.33% of Mo(VI) could be removed after three cycles, in the condition of 10 mg/L initial Mo(VI) concentration and 0.05 mol/L NaOH desorption solution (Fig. 4(b)). These results confirmed that DWTR had a certain potential to be reused for at least three cycles.

3.6. Adsorption mechanism of Mo(VI) on DWTR

3.6.1. Adsorption mechanism characterized by the pH analysis

The variation of aqueous solution pH is a crucial controlling factor in the process of Mo(VI) adsorption. Therefore, the effect of initial pH for Mo(VI) removal with DWTR was investigated and the results are shown in Fig. 5. The process of DWTR for Mo(VI) removal exhibited that the adsorption capacity increased first, climbed the peak, and then followed by a decrease with the further increase of pH in experimental solutions. This similar trend of Mo(VI) adsorption was also observed in other studies [2,6]. It was

Table 4
Thermodynamic parameters for the adsorption of Mo(VI) on DWTR

Temperature (K)	ΔG° (kJ/mol)	ΔH° (kJ/mol)	ΔS° (J/(mol K))	R^2
298	−1.372	5.504	23.133	0.970
308	−1.657			
318	−1.833			

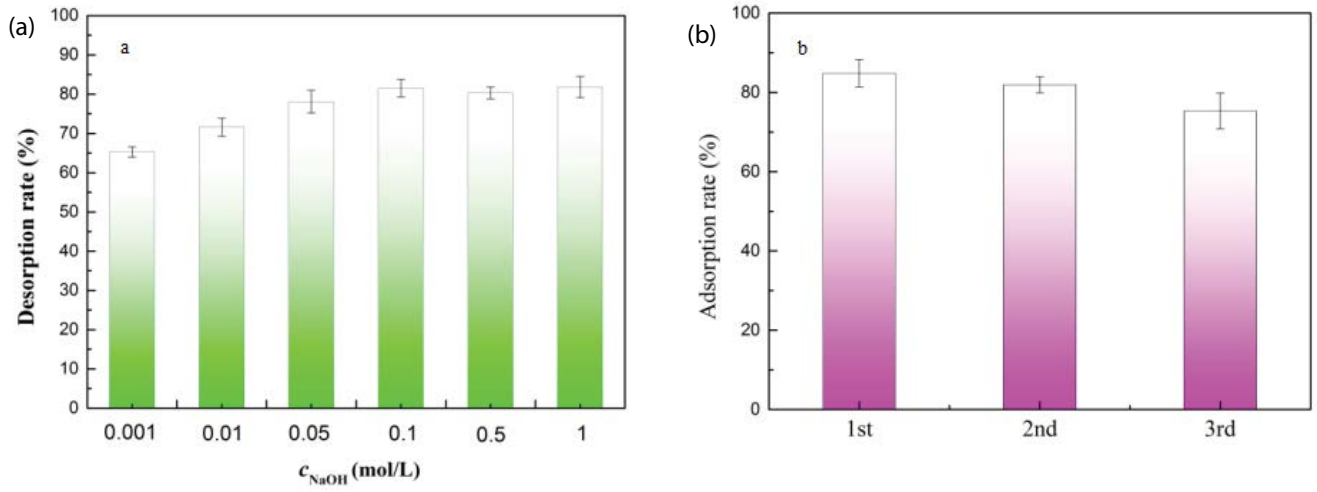

Fig. 4. (a) The percentage of Mo desorption from DWTR after interaction with different NaOH solutions for 5 h at 298 K. (b) Reusability of DWTR. Desorption conditions: 0.05 mol/L NaOH solutions for 5 h at 298 K.

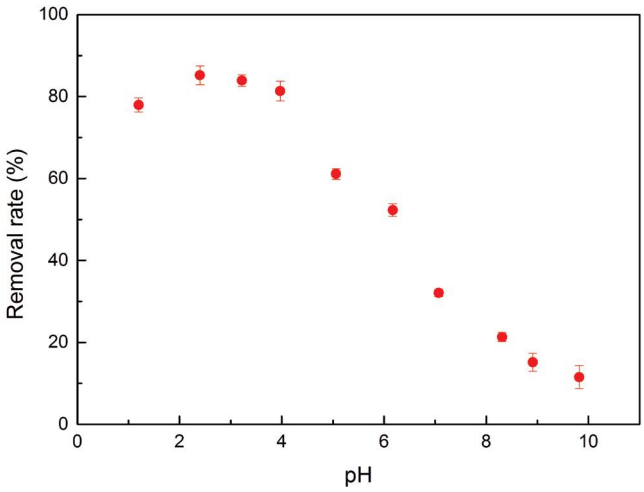

Fig. 5. Effects of varying pH values on Mo(VI) adsorption. Conditions: solid/liquid = 1 g/L, T = 298 K, initial Mo(VI) concentration = 10 mg/L.

apparent that the adsorption of Mo(VI) was considerably influenced by pH values of aqueous solution. The effect of adsorption with pH could be explained by the electrostatic attraction between adsorbent and adsorbate.

The results demonstrate that the maximum amount of Mo(VI) adsorption can be reached when low pH from pH 1.5 to 4.0 can be maintained. Such a maximum removal can be due to the change of Mo(VI) to other species in the pH range 2.0–4.6, such as $Mo_7O_{21}(OH)_3^{3-}$, $Mo_7O_{22}(OH)_2^{4-}$, $Mo_7O_{23}(OH)^{5-}$, and $Mo_7O_{24}^{6-}$ [31]. The lower removal rate at pH < 2.0 may be attributed to the higher concentration of Cl^- anions, which compete with the molybdate anions for interaction with the adsorbent active sites [30,32]. The pH_{PZC} of DWTR was approximately 7.35, and the surface charge of DWTR would be positive at a pH less than the pH_{PZC}. Consequently, at lower pHs, Mo(VI) adsorption would be facilitated by electrostatic attraction. As pH raised above the pH_{PZC}, the surface charge of DWTR became predominantly negative and Mo(VI) adsorption decreased.

However, the proposed explanation is not fully consistent with the presented data, showing a sharp decline of Mo(VI) adsorption far below the pH_{PZC} of DWTR. Therefore, electrostatic attraction is only one part of the explanation for the drop of Mo(VI) adsorption at pH 4.0–7.35. It is explainable and could be rather attributed to the tendency of weak acid adsorption to drop at pH above pH_{PZC} of DWTR.

3.6.2. Adsorption mechanism characterized by the FTIR analysis

The sorption pattern of metals onto materials is attributable to the active groups and bonds present on sorption materials. Therefore, FTIR spectroscopy was employed to identify the functional groups present in the native sorbent (DWTR) and Mo-loaded sorbent (DWTR-Mo) in our study (Fig. 6). The absorption peak around 3,426cm^{-1} can be assigned to stretching vibration of O–H and –NH

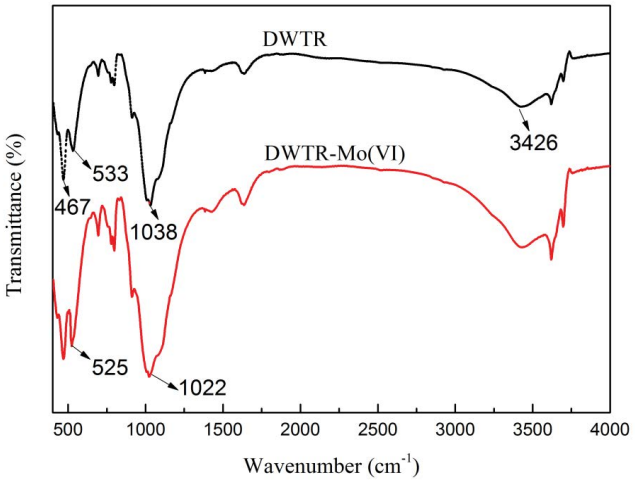

Fig. 6. FTIR spectra of DWTR and DWTR-Mo(VI).

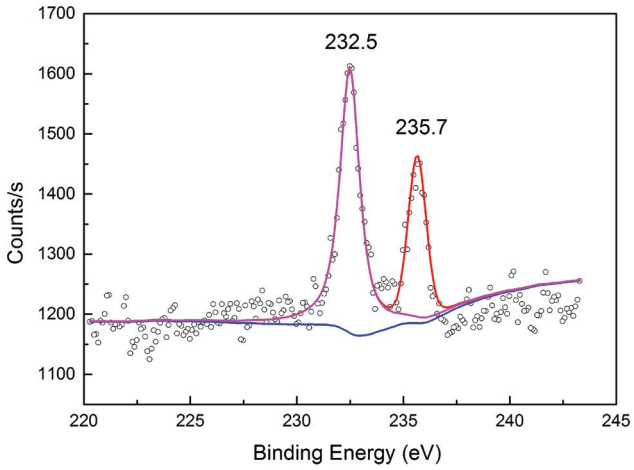

Fig. 7. XPS spectra of the DWTR after Mo(VI) adsorption.

stretching [11]. The peaks around 1,038cm^{-1} were assigned to the Al–OH bands [33]. The bands at 530–540 and 460–470cm^{-1} were assigned to the stretching vibrations of the Fe–O nucleus [34]. After adsorbing Mo(VI), the peaks at 533 and 1,038cm^{-1} shifted to 525 and 1,022cm^{-1}, respectively, which may result from the complexing reaction between Fe(Al)–O group and Mo(VI) [35].

3.6.3. Adsorption mechanism characterized by the XPS analysis

XPS analysis was performed for further verifying the adsorption mechanism inferred by the FTIR analysis. As seen from Fig. 7, the $3d_{3/2}$ and $3d_{5/2}$ spectra of Mo existed at 235.7 and 232.5 eV, respectively, corresponding to the Mo^{6+} state [36]. Obviously, there was no redox reaction in the removal of Mo(VI) onto the DWTR, which further indicated that chemic-sorption and electrostatic attraction existed between Mo(VI) and DWTR. Moreover, the XPS data are in good agreement with FTIR data.

It was reported that Mo(VI) were adsorbed mainly by electrostatic attraction and chemic-sorption [30,37]. In this study, the adsorption of Mo(VI) was considerably influenced by pH values of aqueous solution. Mo(VI) was adsorbed onto the DWTR and there was no other Mo valence state, which were confirmed by the XPS of DWTR-Mo. Furthermore, the change of Al–OH and Fe–O bands in DWTR indicated that adsorption of Mo(VI) was related to Fe and Al. Therefore, it was deduced that the main mechanisms of Mo(VI) adsorption on DWTR should be controlled by electrostatic interaction (physic-sorption) and surface complexation (chemic-sorption) mechanism. The suggested mechanisms of Mo(VI) adsorbed onto DWTR are shown in Fig. 8.

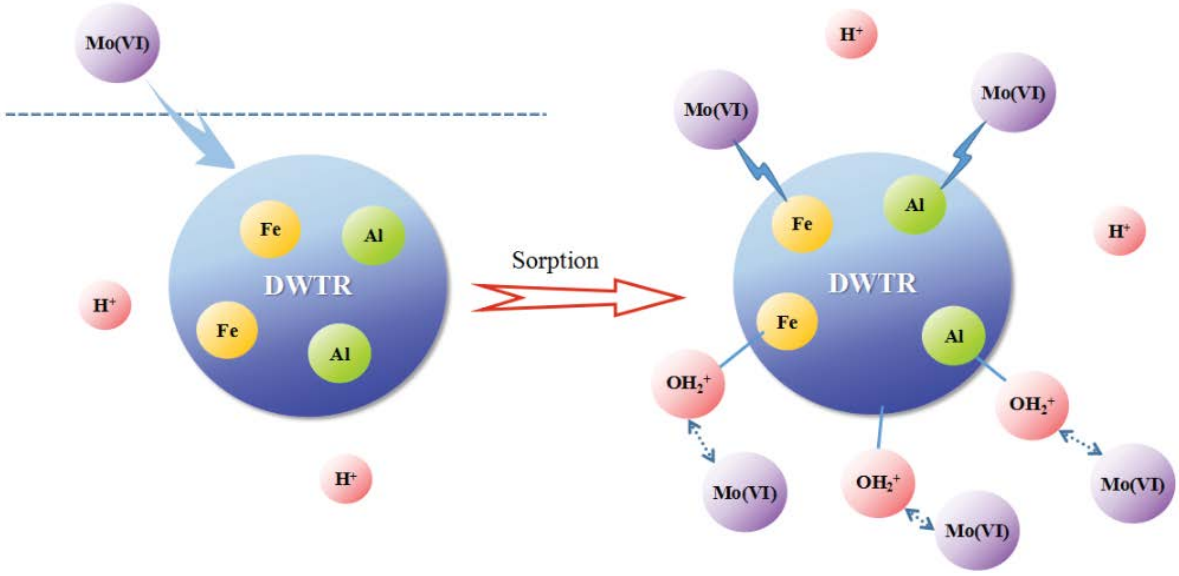

Fig. 8. The suggested mechanism of Mo(VI) adsorbed onto DWTR.

4. Conclusions

The proposed DWTR was fast and efficient for Mo(VI) removal from solutions. The effects of various conditions for the Mo(VI) adsorption were investigated systematically. The sorption process of Mo(VI) followed pseudo-second-order kinetics with 24 h required to reach equilibrium. The sorption isotherm could be fit well by the Langmuir model, and the maximum adsorption capacity reached 31.06 mg/g at 318 K. Thermodynamic parameters revealed that adsorption process was feasible, spontaneous, and endothermic. The desorption/regeneration study revealed that the adsorption sites occupied by Mo could easily be replaced by OH^-, and the DWTR-Mo could be rapidly recovered from the solutions. FTIR and XPS analyses showed that electrostatic interaction and surface complexation were the two major adsorption mechanisms for the sorption of Mo(VI) by DWTR. Results indicate that DWTR could be a suitable and beneficial material for the Mo(VI) removal.

Acknowledgements

This research was supported by the National Natural Science Foundation of China (51709001), the Nature Science Foundation of Anhui Province of China (1708085QD81), and the Youth Foundation of Anhui University of Technology (QZ201520). Constructive comments from anonymous reviewers are highly appreciated.

References

[1] A. Afkhami, A.R. Norooz, Removal, preconcentration and determination of Mo(VI) from water and wastewater samples using maghemite nanoparticles, Colloids Surf., A, 346 (2009) 52–57.
[2] Y.J. Tu, T.S. Chan, H.W. Tu, S.L. Wang, C.F. You, C.K. Chang, Rapid and efficient removal/recovery of molybdenum onto $ZnFe_2O_4$ nanoparticles, Chemosphere, 148 (2016) 452–458.
[3] C. Namasivayam, D. Sangeetha, Removal of molybdate from water by adsorption onto $ZnCl_2$ activated coir pith carbon, Bioresour. Technol., 97 (2006) 1194–1200.
[4] A. Moret, J. Rubio, Sulphate and molybdate ions uptake by chitin-based shrimp shells, Miner. Eng., 16 (2003) 715–722.
[5] M.I.E. Halmi, H. Wasoh, S. Sukor, S.A. Ahmad, M.T. Yusof, M.Y. Shukor, Bioremoval of molybdenum from aqueous solution, Int. J. Agric. Biol., 16 (2014) 848–850.
[6] J.J. Lian, S.G. Xu, N.B. Chang, C.W. Han, J.W. Liu, Removal of molybdenum(VI) from mine tailing effluents with the aid of loessial soil and slag waste, Environ. Eng. Sci., 30 (2013) 213–220.
[7] J.J. Lian, S.G. Xu, Y.M. Zhang, C.W. Han, Molybdenum(VI) removal by using constructed wetlands with different filter media and plants, Water Sci. Technol., 67 (2013) 1859–1866.
[8] I. Polowczyl, P. Cyganowski, B.F. Urbano, B.L. Rivas, M. Bryjak, N. Kabay, Amberlite IRA-400 and IRA-743 chelating resins for the sorption and recovery of molybdenum(VI) and vanadium(V): equilibrium and kinetic studies, Hydrometallurgy, 169 (2017) 496–507.
[9] R. Mamtaz, D.H. Bache, Reduction of arsenic in groundwater by coprecipitation with iron, J. Water Supply Res. Technol., 50 (2001) 313–324.
[10] W.J. Shan, Y.N. Shu, H. Chen, D.Y. Zhang, W. Wang, H.Q. Ru, Y. Xiong, The recovery of molybdenum(VI) from rhenium(VII) on amino-functionalized mesoporous materials, Hydrometallurgy, 165 (2016) 251–260.
[11] Z.N. Lou, J. Wang, X.D. Jin, L. Wan, Y. Wang, H. Chen, W.J. Shan, Y. Xiong, Brown algae based new sorption material for fractional recovery of molybdenum and rhenium from wastewater, Chem. Eng. J., 273 (2015) 231–239.
[12] G.R. Helz, B.E. Erickson, T.P. Vorlicek, Stabilities of thiomolybdate complexes of iron: implications for retention of essential trace elements (Fe, Cu, Mo) in sulfidic waters, Metallomics, 6 (2013) 1131–1140.
[13] C. Freund, A. Wishard, R. Brenner, M. Sobel, J. Mizelle, A. Kim, D.A. Meyer, J.L. Morford, The effect of a thiol-containing organic molecule on molybdenum adsorption onto pyrite, Geochim. Cosmochim. Acta, 174 (2016) 222–235.
[14] J. Jiao, J.B. Zhao, Y.S. Pei, Adsorption of Co(II) from aqueous solutions by water treatment residuals, J. Environ. Sci., 52 (2017) 232–239.
[15] P. Castaldi, M. Silvetti, G. Garau, D. Demurtas, S. Deiana, Copper(I) and lead(II) removal from aqueous solution by water treatment residues, J. Hazard. Mater., 283 (2015) 140–147.
[16] C. Wang, R. He, Y. Wu, M. Lurling, H. Cai, H.L. Jiang, X. Liu, Bioavailable phosphorus (P) reduction is less than mobile P immobilization in lake sediment for eutrophication control by inactivating agents, Water Res., 109 (2016) 196–206.
[17] A.G. Caporale, P. Punamiya, M. Pigna, A. Violante, D. Sarkar, Effect of particle size of drinking-water treatment residuals on the sorption of arsenic in the presence of competing ions, J. Hazard. Mater., 260 (2013) 644–651.
[18] K.D. Quinones, A. Hovsepyan, A.O. Anane, J.C.J. Bonzongo, Insights into the mechanisms of mercury sorption onto aluminum based drinking water treatment residuals, J. Hazard. Mater., 307 (2016) 184–192.
[19] Y.Q. Zhao, L.P. Doherty, D. Doyle, Fate of water treatment residual: an entire profile of Ireland regarding beneficial reuse, Int. J. Environ. Stud., 68 (2011) 161–170.
[20] G.R. Legendre, D.D. Runnells, Removal of dissolved molybdenum from wastewaters by precipitates of ferric iron, Environ. Sci. Technol., 9 (1975) 744–749.
[21] J.S. Noh, J.A. Schwarz, Estimation of the point of zero charge of simple oxides by mass titration, J. Colloid Interface Sci., 130 (1989) 157–164.
[22] D. Kumar, J.P. Gaur, Chemical reaction- and particle diffusion-based kinetic modeling of metal biosorption by a Phormidium sp.-dominated cyanobacterial mat, Bioresour. Technol., 102 (2011) 633–640.
[23] S.S. Gupta, K.G. Bhattacharyya, Adsorption of Ni(II) on clays, J. Colloid Interface Sci., 295 (2006) 21–32.
[24] F. Helfferich, Ion-Exchange, McGrawHills, New York, USA, 1962.
[25] Y.J. Tu, C.F. You, C.K. Chang, T.S. Chan, S.H. Li, XANES evidence of molybdenum adsorption onto novel fabricated nano-magnetic $CuFe_2O_4$, Chem. Eng. J., 244 (2014) 343–349.
[26] Y.C. Chen, C.Y. Lu, Kinetics, thermodynamics and regeneration of molybdenum adsorption in aqueous solutions with NaOCl-oxidized multiwalled carbon nanotubes, J. Ind. Eng. Chem., 20 (2014) 2521–2527.
[27] M.M. EI-Moselhy, A.K. Sengupta, R. Smith, Carminic acid modified anion exchanger for the removal and preconcentration of Mo(VI) from wastewater, J. Hazard. Mater., 185 (2011) 442–446.
[28] B. Verbinnen, C. Block, P. Lievens, A.V. Brecht, C. Vandecasteele, Simultaneous removal of molybdenum, antimony and selenium oxyanions from wastewater by adsorption on supported magnetite, Waste Biomass Valorization, 4 (2013) 635–645.
[29] S. Paikaray, M.J. Hendry, J. Essilfie-Dughan, Controls on arsenate, molybdate, and selenate uptake by hydrotalcite-like layered double hydroxides, Chem. Geol., 345 (2013) 130–138.
[30] C. Namasivayam, M.V. Sureshkumar, Removal and recovery of molybdenum from aqueous solutions by adsorption onto surfactant-modified coir pith a lignocellulosic polymer, Clean–Soil Air Water, 37 (2009) 60–66.
[31] Y. Xiong, C.B. Chen, X.J. Gu, B.K. Biswas, W.J. Shan, Z.N. Lou, D.W. Fang, S.L. Zang, Investigation on the removal of Mo(VI) from Mo-Re containing wastewater by chemically modified persimmon residua, Bioresour. Technol., 102 (2011) 6857–6862.
[32] K.Z. Elwakeel, A.A. Atia, A.M. Donia, Removal of Mo(VI) as oxoanions from aqueous solutions using chemically modified magnetic chitosan resins, Hydrometallurgy, 97 (2009) 21–28.

[33] L.L. Bihan, F. Dumeignil, E. Payen, J. Grimblot, Chemistry of preparation of alumina aerogels in presence of a complexing agent, J. Sol-Gel Sci. Technol., 24 (2002) 113–120.
[34] M. Mohapatra, K. Rout, B.K. Mohapatra, S. Anand, Sorption behavior of Pb(II) and Cd(II) on iron ore slime and characterization of metal ion loaded sorbent, J. Hazard. Mater., 166 (2009) 1506–1513.
[35] A. Pramanik, S. Maiti, S. Mahanty, Superior lithium storage properties of $Fe_2(MoO_4)_3$/MWC -NT composite with a nano-particle (0D)-nanorod (1D) hetero-dimensional morphology, Chem. Eng. J., 307 (2016) 239–248.
[36] E. Yavuz, K.V. Ozdokur, I. Cakar, S. Kocak, F.N. Ertas, Electrochemical preparation, characterization of molybdenum-oxide/platinum binary catalysts and its application to oxygen reduction reaction in weakly acidic medium, Electrochim. Acta, 151 (2015) 72–80.
[37] F.Q. Wang, J.J. Lian, Y.M. Zhang, Batch and column study: adsorption of Mo(VI) from aqueous solutions using $FeCl_2$-modified fly ash, Desal. Wat. Treat., 51 (2013) 5727–5734.